Analog phase holograms by electron beam lithography

Paul D. Maker and Richard E. Muller

Center for Space Microelectronics Technology, Jet Propulsion Laboratory
California Institute of Technology, Pasadena, CA 91109

ABSTRACT

Phase holograms have been have been created on the surface of a thin film of poly-methyl methacrylate (PMMA, Plexiglas) by direct-write electron beam (E-Beam) lithography. The process involves delivering a patterned exposure dose followed by partial development with a strong developer. The patterned dose derives from arbitrary computer-calculated holograms, which must be corrected for the sensitivity characteristic of the PMMA and for the effective point-spread function of the E-Beam.

KEY WORDS: phase-holograms, computer generated holograms, diffractive optics, binary optics

1. INTRODUCTION

Surface-contouring an E-Beam resist by controlling both the exposure dose and the development process was first demonstrated by Fujita[1] in 1981. They fabricated micro Fresnel zone-plates, blazed gratings and Fresnel lenses in poly methylmethacrylate (PMMA) by scanning an electron beam in either straight lines or circles, with the dose adjusted to give the desired etch depth after partial development. Their groove shapes were quite irregular, but devices with 50% to 60% efficiency and near-diffraction-limited performance were produced. More recently Ekberg[2,3] reported on kinoform phase holograms. These were patterns comprising a 512x512 array of 10 μm square pixels, each with a unique E-Beam exposure dose calculated to give the appropriate etch depth upon development. Ten doses/depths were used. Diffraction efficiencies of 70% were reported. In earlier papers[4,5] we reported upon the fabrication, physical, and optical characterization of kinoform lenses that encoded 16-level phase holograms and a Fresnel lens having a diffraction limited focal spot and 83% efficiency. At that time, only an approximate treatment of the E-Beam proximity effect was used. The fabrication imperfections thus introduced caused significant performance degradation. In this paper, we report upon a technique for treating the proximity effect exactly, and upon the performance of an off-axis Fresnel lens and several, more complicated, phase holograms fabricated using the method and all 64 doses that our E-Beam is capable of delivering.

2. EXPERIMENT

In an earlier paper we described the fabrication and testing of a Fresnel lens in PMMA by direct-write, E-Beam lithography. First, the relation between applied E-Beam dose and the amount of PMMA removed in a fixed development period in acetone was determined. It was found that the etch depth was approximately proportional to the development time, that depths of up to 1.5 microns could be reached using a 50 KV electron beam energy, and that in large open areas the depth could be controlled to ± 0.02μm (± λ_{vis}/50 phase delay). The surface-relief pattern of the lens was then encoded at 1 μm intervals over a 3 mm square area, and the E-Beam dose necessary to remove the calculated amount of PMMA was delivered at each pixel. While this lens demonstrated diffraction limited performance and >80% efficiency, its far-field pattern contained a set of diverging, concentric rings of radiation having some 10% of the incident energy. Atomic force microscopy revealed that the resist profile at the boundary between Fresnel zones - properly, an abrupt step function of height $\lambda/(n-1)$ - had a fillet of material remaining in the bottom and a flattened off top. This is due to the well-known E-Beam 'proximity effect' - electrons back-scattered from within the sample lead to a halo of exposure dose surrounding the principle, point-like primary dose. The spatial distribution of this back scatter, or secondary, dose is roughly Gaussian, with an amplitude and width that depend strongly on the substrate material and upon the E-Beam voltage. In order to improve the performance of E-Beam direct-written diffractive optics, it is necessary to carefully characterize and compensate for this effect.

To determine the dose sensitivity of PMMA and the range and amplitude of the proximity effect. we exposed simple test patterns on samples identical to time. that would eventually bear diffractive optical elements. A rectangular pattern 50 x 150 µm was used, exposed at sixteen different doses spanning the range of interest. The samples were 2 µm thick layers of 950K molecular weight PMMA spun from 5% solution in chlorobenzene at 4000 rpm. Five coats were necessary to build up the 2 µm thickness. Ten minute hot plate bake-oats at 170° C were used between coats. In subsequent work, no evidence of interfacial boundaries was evident. Prior to exposure, the samples were ovcl-coated with 5011111 of aluminum which served as a discharge layer during E-Beam exposure. Following exposure, the samples were developed in a manner identical to that used for diffractive optic devices. The horizontally spinning samples were exposed to putt acetone for 1 1.5 seconds delivered downward from a 1 mm diameter orifice by an electronically controlled Tridac dispense head, Instant, vigorous" dry nitrogen blow-off and drying commenced upon termination of acetone delivery. A a electronically controlled Solitec spinner was used. The point of delivery of the acetone coincided with the spin axis, which was carefully chosen to be -1-2 mm from any pattern. This avoided a slight increase in etch rate found to exist directly beneath the acetone delivery point. A1 'M topographic data of the exposed and developed samples was recorded. Fig. 1 illustrates the dose sensitivity of PMMA. Under such aggressive development, the usual high-gamma characteristic of E-Beam exposed I'MMA is completely absent. All that remains is a first order dissolution process characterized by exponential dependence of developed depth upon delivered dose. Using this sensitivity data, the profile of PMMA removed from these samples could be inverted to give a a effect i ve deli vered dose. Since the dose response function was determined by measuring the amount of PMM A removed at the center of the. exposed area, all inferred doses are in terms Of the total delivered dose, primary plus integrated secondary. Fig. 2 shows typical data, giving the inferred dose as a function of distance across the 50 micros width of the test pattern. This curve reveals by inspection the role of primary and secondary doses. The sudden jumps seal 50 and 100 µm are due to the primary dose, while the adjacent, sloped regions represent the effect of the back scattered or secondary dose.. A 1 Digital Instruments Nanoscope III Scanning Probe Microscope (SPM) was used in contact II)()(Ic to record AFM data.

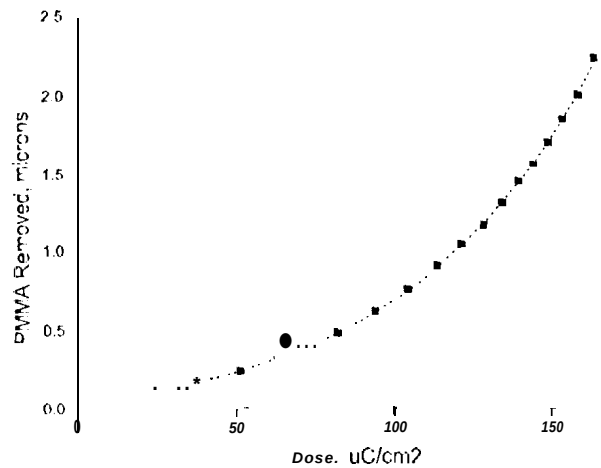

Fig.]. Dose response of I'MMA fitted to a putt exponential, a + b*exp(D/c) where a = -0.11 ± .02 µm, b , (). 15±.01 µm and d = 60.8±1 .0 µC/cm^2. The standard deviation of the fit was .010 µm.

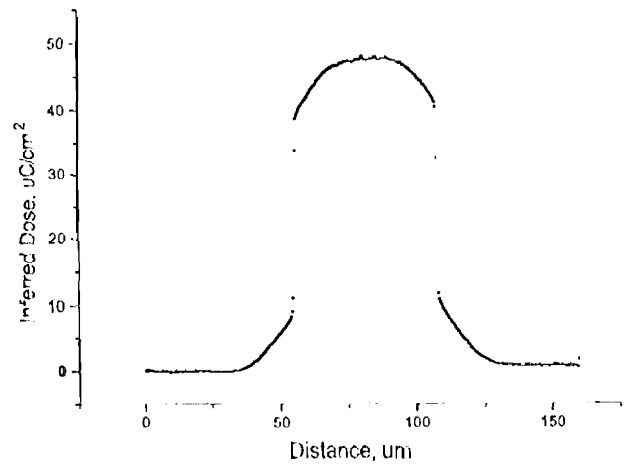

] ig. 2. Inferred total dose from AFM data and dose response function of Fig. I.

The spatial dependence of the E-Beam point spread function - primary plus secondary dose - can be taken as $PSF(\vec{r}) = \delta(\vec{r}) + \frac{\eta}{\pi\alpha^2} \exp(-\vec{r}^2/\alpha^2)$ where η is its amplitude, α is its range, and δ is the Dirac delta function. This can be integrated directly. For instance, if x is the direction normal to a half-plane of uniform dose, the secondary dose falls off as $Dsec(x) = \frac{\eta}{2} Dprim \times erfc(x/\alpha)$ where erfc() is the complementary error function. 1 ig. 3 shows a fit of the central region of Fig. 2 to a compound error function.

Similar data was taken for all of the test patterns. Results are summarized in Fig. 4. The proximity range was found to be independent of dose within experimental error - α = 8.0 ± 0.2 μm. The proximity effect amplitude is seen to vary between 0.4 to 0.5 for doses between 20 to 140 μC/cm 2, the range anticipated in fabrication 01 diffractive optic devices. While this variation is somewhat larger than the measurement uncertainty, for purposes of modeling, it has been ignored, and the mean value, 0.4 ± 0.05, is used in what follows.

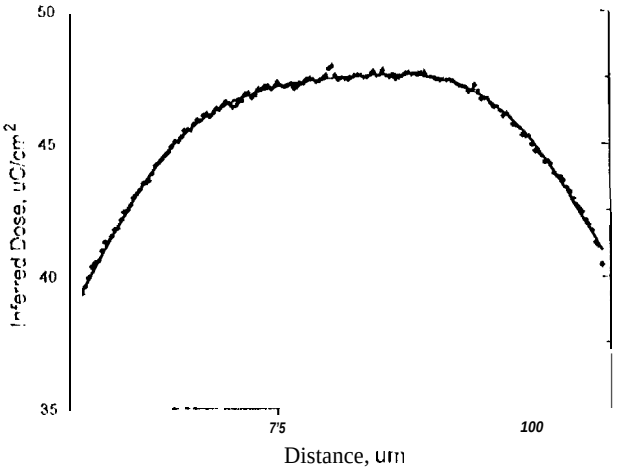

Fig. 3. Data of Fig. 2 fit to complementary error functions plus a linear term. Derived values for the proximity effect range and amplitude are 8.12:10.0711111 and 0.47 ± 0.05.

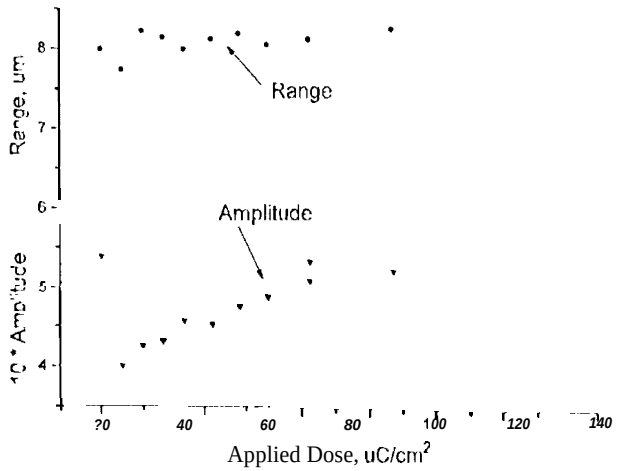

Fig. 4. Summary of proximity effect range and amplitude data for all test patterns.

Continuing the above. train of thought, we can describe the total dose delivered to the sample as a convolution of the primary dose pattern with the 1 E-Beam point spread function. If $D_{prim}(\vec{r})$ is the delivered primary dose and $D_{tot}(\vec{r})$ the total exposure dose due to 1)(1), then $D_{tot}(\vec{r}) = \iint D_{prim}(\vec{r}_o) \times PSF(\vec{r} - \vec{r}_o) \times \partial(\vec{r} - \vec{r}_o) = D_{prim}(\vec{r}) \otimes PSF(\vec{r})$. With this formulation, it is clear that the proximity effect can be corrected by deconvolving the point spread function from tbc desired pattern prior to exposing il. Deconvolution by Fourier transform Ic.presents a straightforward way to do this. If $P(\vec{r})$ is the desired exposure pattern and $P(\vec{k})$ its Fourier transform, and $PSF(\vec{r})$ is the point spread function and $PSF(\vec{k})$ its Fourier transform, then $Pc(\vec{k})$, the Fourier transform of the corrected exposure pattern is given by $Pc(\vec{k}) = P(\vec{k}) / PSF(\vec{k})$. $Pc(\vec{r})$ is then obtained by inverse transforming $Pc(\vec{k})$. This procedure results in regions in which $Pc(\vec{r})$ is negative. In many situations, this means that an exact deconvolution solution is not physically realizable. In the present case, negative doses can be eliminated by first recessing, or biasing, the starting data. Typical patterns require about -O.? μm of bias. A care.fully optimized two dimensional fast Fourier transform deconvolution program has been implemented on our VAX Station 3100 computer. It handles the 4K by 4K problem in five hours. Additional software distributes (he. doses into 64 equally spaced 'shot rank' values, writes the shot rank table needed by the E-Beam control file, and finally writes the pattern data file in native E-Beam for Inst. The pattern file for a general 4K by 4K phase. hologram is some 250 MB long.

The E-Beam machine used was the JEOL JBX-5DII. It was operated at its maximum beam voltage, 50 KV, so as to maximize the usable etch depth in PMMA. The incident electron beam is scattered and slowed as it penetrates, eventually dissipating some 5 μm into PMMA. As the slowed electrons are actually more effective in breaking bonds, the general effect is a mushroom-shaped exposure volume. The proximity effect is thus highly depth dependent, and only near the surface - within the top 1 -2 μm - do the approximations used in the above development remain valid. Further, this limits the usefulness of E-Beam direct write phase holograms, as described her c, to visible light wavelengths for transmission dc.vices and to near-IR for reflective devices.

In writing the holograms, an E-Beam diameter roughly 1/5 the pixel size is used. It was rastered over the pixel in a 10x 10 pattern. The beam is blanked between successive elementary patterns, which in this case are the square pixels which differ

only in their shot rank. By adjusting the beam's F/# (using a set of fixed apertures) its current density is raised until the dwell time at each raster point equals the minimum dwell time for the E-Beam scanning circuitry (0.5 μs) for the minimum dose called out in the pattern data. Under these conditions, pixels could be written at the rate of 10^5 per second, independent of pixel sire. This exposure method - scanning a Gaussian shaped beam over each pixel and then indexing to the next pixel - inevitably leads to some small non uniformity in the exposure. dose. Blanking errors also contribute to exposure non uniformity. As discussed later, this presents another limitation to the usefulness of direct-wr'ik E-Beam phase holograms.

Another source of exposure uniformity error, and a systematic one, is field stitching error. The JEOL machine was operated using its low resolution, long focal length objective lens. It could scan an 800 μm field, '1'0 limit deflector distortion, the field was in fact kept smaller than 400" pill. Stage movement repositioned the sample upon completion of the exposure within a field. The stage position is determined interferometrically, but per feet positioning is not possible and field stitching errors are unavoidable. The factory spec is ±70 nm 3σ. Further, the E-Beam deflectors must be calibrated to exactly span a field. To assure this, our samples had on Illc.in a gold fiducial cross. This cross, rather than one on the E-Beam stage, was used for the (automat ic) deflector calibration procedure. 1 Evidence of residual field stitching and calibration error can be found in all of our devices. Since positioning the fiducial on the sample, the problem is much reduced, but it represents the limiting factor when attempting to construct holograms in which coherence over large areas is essential.

3. INDIVIDUAL DEVICES

Several devices have been fabricated using the above procedures. An off-axis Fresnel lens was produced. It was 3 mm square, had a 38 mm focal length, and was 2 mm off-axis. With these parameters and a 0.8 μm square pixel, its outermost Fresnel zones were a minimum of eight pixels wide. The lens demonstrated diffraction limited focusing performance, with 88% of the incident energy passing through the focal spot. Of the remainder, 1 .6% went into the zeroth order, <2% went into higher focusing orders, <1% went into coherent diffract ion by irregularities at the pixel boundaries, <1% went into cobc.rent diffraction by the field stitching errors, and ~ I 0% went into incoherent diffuse scattering arising from general surface roughness. RMS surface roughness from AFM data was 0.0? μm.

A 15x 15 optical fan-out device - one collimated input laser beam, 225 output collimated beams fanning our in a regular 15x15 array - was fabricated. It was designed by '1'. C. Chao and his coworkers at JPL. The repeat unit was 44 μm square. Its theoretical efficiency was ~80% with ±10% intensity variation from beam to beam. '1 'he fabricated device had an efficiency of ~60% and a ± 25% beam to beam variation. The device used 2 μm pixels and was 1 in square. E-Beam expose time was 37 hr.

A. Gmitro and his coworkers at the University of Arizona, using their Gerchberg-Saxton preconditioned random search algorithm, designed 128x128 pixel phase holograms that produced on-axis images of the numerals 1 through 9. Written with 2 μm pixels, they were arrayed 4x4 to produce 1 mm square devices. The salient feature of these devices is the total absence of order in the holograms. On a local scale, the pixel to pixel variation in phase seems to be a random number between 0 and 2π. Yet they performed well, with ~70% of the total transmitted intensity going into the designed pattern while the undiffracted beam had ~2.5% of the transmitted energy. Intensity variation amongst the 'on' pixels was ~25%, while 'off' pixels were on average 3% as bright as an average 'on' pixel. This device was written on a substrate lacking an integral fiducial cross, and it is expected that performance will improve using the new substrates. Lateral etching of exposed pixel sidewalls undoubtedly accounts for a large part of the performance shortfall for this and like devices.

Most recently, a small reflective imaging grating for use in an imaging spectrometer having a focal plane array detector has been fabricated, Using 4K x 4K 0.5 μm pixels, the 2 mm square device accepted radiation from a 10 cm distant point source and imaged it back upon itself but displaced off axis by 1 cm. Dispersion was adjusted to spread the desired spectral region across the focal plane detector. This was done by tilting the grating to adjust the angle of incidence. The average grating spacing was ~5 μm. AFM topographic data is shown in Fig. 5. The grove profile is extremely accurate, with very flat smrl'aces. Roughness persists, but over a 4.5 μm by 15 μm area on a grove flat, total surface variation was only 6 nm RMS. Being a reflective device, this corresponds to a phase variation of only λ/50. At the design wavelength, 633 nm, its diffraction efficiency was measured to be >90%.

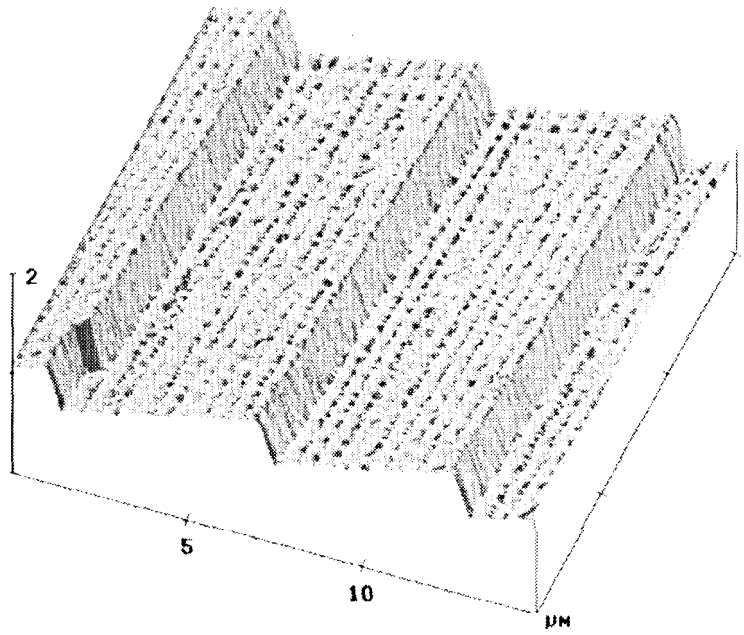

Fig. 5. AFM topograph of imaging grating. The RMS deviation of the groove flats from planar surfaces is 6 nm.

4. CONCLUSIONS

The results obtained indicate that direct write, partial exposure E-Beam lithography can produce excellent transmissive and reflective optical elements for use in the visible. Efforts are under way to reduce the diffuse scattering and to develop algorithms to corral for the effects of side wall etching. It should be noted that sub-pixel structure is effectively averaged out in the forward direction. If the spatial extent of the holographic image is restricted, the approximation that only the pixel-averaged phase delay is valid. In that case, material etched from side walls can be compensated for by reducing the pixel depth. It should also be noted that exposure times for theses devices are limited by the speed of the pattern generator. Plans call for upgrading ours by a factor of three.

5. ACKNOWLEDGMENTS

The research described in this paper was performed by the Center for Space Microelectronics Technology, Jet Propulsion Laboratory, California Institute of Technology, and was jointly sponsored by the Ballistic Missile Defense organization / innovative Science and Technology Office and the National Aeronautics and Space Administration / Office of Advanced Concepts and Technology.

6. REFERENCES

1. T. Fujita, H. Nishihara, and J. Koyama, "Fabrication of micro lenses using electron-beam lithography," *Opt. Lett. 6*, 613-615, 1981.
2. M. Ekberg, M. Larsson, S. Hård, and B. Nilsson, "Multilevel phase holograms manufactured by electron beam lithography," *Opt. Lett. 15*, 568-569, 1990.
3. M. Larsson, M. Ekberg, F. Nikolajeff, and S., Hard, P. D. Maker, and R. E. Muller, "Proximity-compensated kinoforms directly written by e-beam lithography," *SPIE Proceedings Vol. CR49*, July 1993.
4. P. D. Maker, and R. E. Muller, "Phase holograms in polymethylmethacrylate," *J. Vac. Sci. Technol. B 10*, 2516-2519, Nov/Dec1992

[5] P. D. Maker and R. E. Muller, "Phase holograms in PMMA with proximity effect correction," NASA CP-3227, 207-221, Feb. 1993.

[6] P. E. Keller and A. F. Gmitro, "Design and analysis of fixed planar holographic interconnects for optical neural networks," *Appl. Opt.* 31, 5517, 1992.